

Electronic supplementary information

Novel triphenyltin(IV) compounds with carboxylato N-functionalized 2-quinolones as promising potential anticancer drug candidates: *In vitro* and *in vivo* evaluation

Marijana P. Kasalović,^{1,2} Sanja Jelača,³ Žiko Milanović,⁴ Danijela Maksimović-Ivanić,³ Sanja Mijatović,³ Jelena Lađarević,⁵ Bojan Božić,⁶ Zoran Marković,⁴ Tobias Rüffer,⁷ Robert Kretschmer,⁷ Goran N. Kaluđerović,^{*1} Nebojša Đ. Pantelić ^{*8}

¹ Department of Engineering and Natural Sciences, University of Applied Sciences Merseburg, Eberhard-Leibnitz-Straße 2, 06217 Merseburg, Germany

² Department of Chemistry, Faculty of Science, University of Kragujevac, Radoja Domanovića 12, 34000 Kragujevac, Serbia

³ Department of Immunology, Institute for Biological Research "Siniša Stanković" National Institute of Republic of Serbia, University of Belgrade, Bulevar despota Stefana 142, 11060 Belgrade, Serbia

⁴ Department of Science, Institute for Information Technologies, University of Kragujevac, Jovana Cvijića bb, 34000 Kragujevac, Serbia

⁵ Faculty of Technology and Metallurgy, University of Belgrade, Karnegijeva 4, 11000 Belgrade, Serbia

⁶ Institute of Physiology and Biochemistry "Ivan Djaja", Faculty of Biology, University of Belgrade, Studentski trg 16, 11000 Belgrade, Serbia

⁷ Institute of Chemistry, Chemnitz University of Technology, Straße der Nationen 62, D-09111 Chemnitz, Germany

⁸ Department of Chemistry and Biochemistry, Faculty of Agriculture, University of Belgrade, Nemanjina 6, 11080 Belgrade, Serbia

Corresponding authors, E-mail addresses: pantelic@agrif.bg.ac.rs (N.Đ. Pantelić);
goran.kaluderovic@hs-merseburg.de (G.N. Kaluđerović)

TABLE OF CONTENTS OF SUPPLEMENTARY MATERIAL

This supplementary material contains:

- 1) **Table S1.** The experimental and theoretical determinate bond distances (\AA) of the investigated compounds at the DFT/B3LYP-D3BJ/6-311+G(d,p)/ def2-TZVPD level of theory
- 2) **Table S2.** The experimental and theoretical determinate bond angle ($^{\circ}$) of the investigated compounds at the DFT/B3LYP-D3BJ/6-311+G(d,p)/ def2-TZVPD level of theory
- 3) **Table S3.** The experimental and theoretical determinate dihedral angles ($^{\circ}$) of the investigated compounds at the DFT/B3LYP-D3BJ/6-311+G(d,p)/ def2-TZVPD level of theory
- 4) **Table S4.** The calculated Bond Critical Points (BCP) properties at the DFT/B3LYP-D3BJ/6-311+G(d,p)/ def2-TZVPD level of theory: the electron density ($\rho(r)$) and its Laplacian ($\nabla^2\rho(r)$); the Lagrangian kinetic electron density ($G(r)$) and the potential electron density ($V(r)$); the density of the total energy of electrons ($H(r)$) – Cremer-Kraka electronic energy density; the interatomic bond energy, E_{bond} .
- 5) **Table S5.** The experimental and theoretical wavelengths (cm^{-1}) and PED (%) analysis parameters for **Ph₃SnL1**
- 6) **Table S6.** The experimental and theoretical wavelengths (cm^{-1}) and PED (%) analysis parameters for **Ph₃SnL2**
- 7) **Table S7.** The experimental and theoretical wavelengths (cm^{-1}) and PED (%) analysis parameters for **Ph₃SnL3**
- 8) **Table S8.** The experimental and calculated chemical shifts (ppm) in the ¹H NMR newly synthesized triphenyltin(IV) complexes
- 9) **Table S9.** The experimental and calculated chemical shifts (ppm) in the ¹³C NMR newly synthesized triphenyltin(IV) complexes
- 10) **Table S10.** Crystal data and structure refinement for **Ph₃SnL1** and **Ph₃SnL2**
- 11) **Figure S1.** FT-IR spectra of triphenyltin(IV) complexes
- 12) **Figure S2 – S4.** ¹H, ¹³C and ¹¹⁹Sn NMR of triphenyltin(IV) complexes
- 13) **Figure S5.** Structures of newly synthesized compounds with defined characteristics and numbered Bond Critical Points (BCP) obtained by using QTAIM analysis
- 14) **Figure S6 – S7.** Thermogravimetric analyses carried out in a non-inert atmosphere (O_2) and an inert (Ar)
- 15) **Figure S8.** UV-Vis spectra for determination of stability of the complexes
- 16) **Figure S9.** The effect of compounds **Ph₃SnL1**, **Ph₃SnL2** and **Ph₃SnL3** on viability of peritoneal exudate cells
- 17) **Figure S10-S11.** Cell viability
- 18) **Figure S12.** Production of ROS/RNS in A375 and B16 cells

Table S1. The experimental and theoretical determinate bond distances (\AA) of the investigated compounds at the DFT/B3LYP-D3BJ/6-311+G(d,p)/ def2-TZVPD level of theory.

Bond distance (\AA)	Ph₃SnL1		Bond distance (\AA)	Ph₃SnL2		Ph₃SnL3
	exp	theor		exp	theor	
N1-C2	1.377	1.404	N1-C2	1.368	1.404	1.410
C2-C3	1.435	1.450	C2-C3	1.435	1.454	1.448
C2-O3	1.264	1.236	C2-O3	1.259	1.234	1.224
C3-C4	1.435	1.357	C3-C4	1.354	1.358	1.359
C5-C6	1.409	1.409	C5-C6	1.371	1.387	1.387
C6-C7	1.374	1.386	C6-C7	1.392	1.400	1.402
C8-C9	1.379	1.388	C8-C9	1.402	1.409	1.409
C9-C10	1.406	1.409	C9-C10	1.411	1.421	1.418
C10-N1	1.403	1.399	C9-N1	1.396	1.394	1.392
C4-C5	1.448	1.450	C10-C4	1.440	1.450	1.443
C4-C14	1.505	1.505	C4-C13	1.497	1.505	1.361
C10-C5	1.410	1.409	C10-C5	1.414	1.409	1.407
C7-C8	1.383	1.399	N1-C12	1.462	1.458	1.457
C12-C11	1.502	1.510	C12-C11	1.529	1.529	1.528
C11-O1	1.300	1.316	C11-O1	1.289	1.312	1.311
C11-O2	1.226	1.235	C11-O2	1.224	1.228	1.229
O1-Sn1	2.139	2.090	O1-Sn1	2.137	2.057	2.061
Sn1-C15	2.138	2.132	Sn1-C14	2.138	2.127	2.137
C15-C16	1.399	1.403	C14-C15	1.390	1.404	1.404
C16-C17	1.389	1.397	C15-C16	1.391	1.397	1.397
C17-C18	1.386	1.398	C16-C17	1.384	1.398	1.399
C18-C19	1.386	1.398	C17-C18	1.383	1.397	1.397
C19-C20	1.390	1.403	C18-C19	1.390	1.398	1.398
C20-C15	1.395	1.403	C19-C14	1.393	1.403	1.403
Sn1-C21	2.128	2.138	Sn1-C20	2.115	2.135	2.127
C21-C22	1.395	1.403	C20-C21	1.394	1.403	1.403
C22-C23	1.387	1.398	C21-C22	1.386	1.398	1.397
C23-C24	1.391	1.398	C22-C23	1.377	1.399	1.398
C24-C25	1.377	1.398	C23-C24	1.378	1.397	1.397
C25-C26	1.386	1.397	C24-C25	1.389	1.398	1.398
C26-C21	1.398	1.404	C25-C20	1.392	1.403	1.403
Sn1-C27	2.144	2.145	Sn1-C20	2.115	2.135	2.134
C27-C28	1.400	1.404	C26-C27	1.392	1.404	1.404
C28-C29	1.394	1.398	C27-C28	1.393	1.399	1.399
C29-C30	1.392	1.398	C28-C29	1.388	1.398	1.398
C30-C31	1.381	1.397	C29-C30	1.383	1.398	1.398
C31-C32	1.394	1.398	C30-C31	1.388	1.397	1.397
C32-C27	1.389	1.404	C31-C26	1.390	1.404	1.404
MAE	-	0.112	MAE	-	0.014	-
R	-	0.997	R	-	0.997	-

Table S2. The experimental and theoretical determinate bond angle ($^{\circ}$) of the investigated compounds at the DFT/B3LYP-D3BJ/6-311+G(d,p)/ def2-TZVPD level of theory.

Bond angle ($^{\circ}$)	Ph₃SnL1		Bond angle ($^{\circ}$)	Ph₃SnL2		Ph₃SnL3
	exp	theor		exp	theor	theor
N1-C2-O3	118.6	120.2	N1-C2-O3	119.8	121.0	120.7
N1-C2-C3	117.5	116.5	N1-C2-C3	117.3	115.8	116.0
C2-C3-C4	122.5	123.2	C2-C3-C4	122.7	123.4	121.9
C3-C4-C14	121.3	120.7	C3-C4-C13/OH	120.7	120.8	123.4
C4-C5-C6	123.0	121.6	C4-C10-C5	122.4	122.4	122.3
C6-C7-C8	120.2	119.0	C5-C6-C7	120.3	119.3	119.3
C7-C8-C9	120.6	120.8	C6-C7-C8	120.6	120.6	121.0
C8-C9-C10	120.1	120.9	C8-C9-N1	120.8	120.8	121.3
C9-C10-N1	120.8	122.1	C8-C9-C10	119.9	119.3	118.5
N1-C13-C12	108.0	113.0	N1-C12-C11	114.3	111.2	111.8
C12-C11-O1	116.0	115.5	C12-C11-O1	115.3	113.1	113.7
O1-C11-O2	123.7	121.3	O1-C11-O2	126.8	124.5	124.3
C11-O1-Sn1	111.8	107.9	C11-O1-Sn1	124.8	117.4	115.9
O1-Sn1-C15	88.0	95.9	O1-Sn1-C14	95.4	107.8	105.6
O1-Sn1-C21	92.4	110.2	O1-Sn1-C20	97.7	106.5	108.5
O1-Sn1-C27	101.3	110.0	O1-Sn1-C26	89.9	95.8	96.1
C15-Sn1-C21	114.7	109.2	C14-Sn1-C20	122.4	119.1	120.1
C15-Sn1-C27	112.9	110.4	C14-Sn1-C26	115.4	115.3	107.8
C21-Sn1-C27	130.5	118.7	C20-Sn1-C26	120.4	109.2	115.6
Sn1-C15-C16	121.9	122.2	Sn1-C14-C15	120.1	123.1	123.6
Sn1-C15-C20	118.0	118.5	Sn1-C14-C19	121.5	117.6	117.3
C15-C16-C17	120.9	120.2	C14-C15-C16	121.1	120.2	120.2
C16-C17-C18	120.1	119.8	C15-C16-C17	119.9	120.2	120.3
C17-C18-C19	119.7	119.9	C16-C17-C18	119.8	119.9	119.8
C18-C19-C20	120.0	120.4	C17-C18-C19	119.9	119.9	120.0
C19-C20-C15	121.0	119.4	C18-C19-C14	121.1	120.5	120.5
Sn1-C21-C22	123.1	122.1	Sn1-C20-C21	121.4	121.1	121.0
Sn1-C21-C26	119.1	118.5	Sn1-C20-C25	119.8	119.4	119.5
C21-C22-C23	120.8	120.2	C20-C21-C22	120.4	120.0	120.1
C22-C23-C24	120.3	120.3	C21-C22-C23	120.3	120.2	120.2
C23-C24-C25	119.5	119.8	C22-C23-C24	120.1	120.0	120.0
C24-C25-C26	120.1	119.7	C23-C24-C25	119.9	119.9	119.9
C25-C26-C21	121.3	119.1	C24-C25-C20	120.6	120.3	120.3
Sn1-C27-C28	118.3	118.0	Sn1-C26-C27	121.1	122.2	122.5
Sn1-C27-C32	123.4	122.8	Sn1-C26-C31	120.4	118.7	118.4
C27-C28-C29	120.7	120.6	C26-C27-C28	120.9	120.6	120.6
C28-C29-C30	120.3	120.0	C27-C28-C29	120.1	120.0	120.0
C29-C30-C31	119.0	119.8	C28-C29-C30	119.4	119.9	119.9
C30-C31-C32	120.7	120.3	C29-C30-C31	120.4	120.2	120.1
C31-C32-C27	120.8	120.2	C30-C31-C26	121.0	120.4	120.5
MAE	-	2.170	MAE	-	1.918	-
R	-	0.868	R	-	0.881	-

Table S3. The experimental and theoretical determinate dihedral angles ($^{\circ}$) of the investigated compounds at the DFT/B3LYP-D3BJ/6-311+G(d,p)/ def2-TZVPD level of theory.

Dihedral angles ($^{\circ}$)	Ph₃SnL1		Dihedral angles ($^{\circ}$)	Ph₃SnL2		Ph₃SnL3
	exp	theor		exp	theor	theor
N1-C2-C3-C4	0.6	2.2	N1-C2-C3-C4	1.2	2.4	2.6
C2-C3-C4-C14	179.1	178.4	C2-C3-C4-C14	174.5	177.8	177.8
C2-C3-C4-C5	0.1	1.3	C2-C3-C4-C10	-3.5	-1.7	-1.8
C3-C4-C5-C6	179.1	179.7	C3-C4-C10-C5	-178.0	-179.1	-178.8
C3-C4-C5-C10	0.2	0.6	C3-C4-C10-C9	3.0	0.0	0.0
C4-C5-C6-C7	179.3	179.2	C4-C10-C5-C6	-179.0	-178.8	-178.5
C5-C6-C7-C8	-0.6	-0.7	C10-C5-C6-C7	-0.2	-0.5	-0.7
C6-C7-C8-C9	1.8	1.0	C5-C6-C7-C8	0.3	0.1	0.2
C7-C8-C9-C10	-1.0	-0.1	C6-C7-C8-C9	-0.4	-0.4	-0.7
C8-C9-C10-C5	-1.1	-1.2	C7-C8-C9-C10	0.2	0.6	-1.6
N1-C13-C12-C11	156.7	50.8	N1-C12-C11-O1	-11.5	-28.9	-26.0
C12-C11-O1-Sn1	164.4	166.7	C12-C11-O1-Sn1	169.0	157.3	160.4
C11-O1-Sn1-C15	-172.2	-174.4	C11-O1-Sn1-C14	81.7	79.0	-53.4
C11-O1-Sn1-C21	-57.4	-72.7	C11-O1-Sn1-C20	-42.1	-49.8	76.7
C11-O1-Sn1-C27	74.8	60.7	C11-O1-Sn1-C26	-162.8	-160	-163.7
O1-Sn1-C15-C16	101.4	173.0	O1-Sn1-C14-C15	-17.7	-62.3	66.6
O1-Sn1-C15-C20	-75.5	6.6	O1-Sn1-C14-C19	155.6	117.6	-112.3
Sn1-C15-C16-C17	-177.1	-178.7	Sn1-C14-C15-C16	172.8	179.3	178.6
C15-C16-C17-C18	-1.1	0.3	C14-C15-C16-C17	0.4	0.1	0.5
C16-C17-C18-C19	0.5	0.4	C15-C16-C17-C18	0.2	0.4	0.2
C17-C18-C19-C20	1.4	0.5	C16-C17-C18-C19	-0.7	0.2	-0.2
C18-C19-C20-C15	-2.6	0.0	C17-C18-C19-C14	0.4	0.2	0.4
C19-C20-C15-Sn1	179.0	178.8	C18-C19-C14-Sn1	-173.1	-179.1	-179.1
O1-Sn1-C21-C22	126.5	72.7	O1-Sn1-C20-C21	87.4	67.3	-69.3
O1-Sn1-C21-C26	-54.6	-109.3	O1-Sn1-C20-C25	-96.5	-112.5	111.3
Sn1-C21-C22-C23	177.8	177.9	Sn1-C20-C21-C22	175.0	179.6	179.3
C21-C22-C23-C24	-0.5	0.0	C20-C21-C22-C23	0.9	0.5	0.1
C22-C23-C24-C25	1.3	0.1	C21-C22-C23-C24	0.1	0.4	0.3
C23-C24-C25-C26	-0.7	-0.2	C22-C23-C24-C25	-0.9	-0.1	0.2
C24-C25-C26-C21	-0.9	0.1	C23-C24-C25-C20	0.8	0.4	0.1
C25-C26-C21-Sn1	-177.2	-177.9	C24-C25-C20-Sn1	-175.9	-179.8	-179.2
O1-Sn1-C27-C28	114.3	120.4	O1-Sn1-C26-C27	-137.7	-174.7	-165.8
O1-Sn1-C27-C32	-63.7	-63.2	O1-Sn1-C26-C31	36.5	7.9	18.7
Sn1-C27-C28-C29	-177.2	175.5	Sn1-C26-C27-C28	174.0	177.5	175.7
C27-C28-C29-C30	-2.3	0.7	C26-C27-C28-C29	0.5	0.1	0.4
C28-C29-C30-C31	1.2	1.2	C27-C28-C29-C30	0.6	0.1	0.1
C29-C30-C31-C32	1.3	0.5	C28-C29-C30-C31	-1.1	0.1	0.1
C30-C31-C32-C27	-2.7	-1.2	C29-C30-C31-C26	0.6	0.2	0.2
C31-C32-C27-Sn1	179.5	176.0	C30-C31-C26-Sn1	-173.8	-177.7	-175.6
MAE	-	11.226	MAE	-	0.699	-
R	-	0.965	R	-	0.993	-

Table S4. The calculated Bond Critical Points (BCP) properties at the DFT/B3LYP-D3BJ/6-311+G(d,p)/ def2-TZVPD level of theory: the electron density ($\rho(r)$) and its Laplacian ($\nabla^2\rho(r)$); the Lagrangian kinetic electron density ($G(r)$) and the potential electron density ($V(r)$); the density of the total energy of electrons ($H(r)$) – Cremer-Kraka electronic energy density; the interatomic bond energy, E_{bond} .

Critical points	$\rho(r)$ (a.u)	$\nabla^2 \rho(r)$ (a.u)	$G(r)$ (kJ mol ⁻¹)	$V(r)$ (kJ mol ⁻¹)	$H(r)$ (kJ mol ⁻¹)	$-(G(r)/(V(r))$	E_{bond} (kJ mol ⁻¹)
Ph₃SnL1							
BCP-1	0.109	0.106	195.1	-320.7	-125.6	0.61	-160.4
BCP-2	0.108	0.119	200.9	-323.8	-122.9	0.62	-161.9
BCP-3	0.111	0.109	199.6	-327.5	-127.9	0.61	-163.8
BCP-4	0.090	0.359	278.0	-320.4	-42.4	0.87	-160.2
BCP-1'	0.013	0.048	28.4	-25.6	2.9	1.11	-12.8
BCP-2'	0.010	0.035	19.9	-16.8	3.1	1.18	-8.4
Ph₃SnL2							
BCP-1	0.112	0.109	202.1	-332.7	-130.6	0.61	-166.4
BCP-2	0.110	0.114	202.7	-330.3	-127.7	0.61	-165.2
BCP-3	0.110	0.110	198.7	-325.3	-126.6	0.61	-162.6
BCP-4	0.095	0.403	310.4	-356.1	-45.7	0.87	-178.0
BCP-1'	0.010	0.035	20.4	-17.5	2.9	1.17	-8.8
BCP-2'	0.008	0.027	15.6	-13.2	2.4	1.19	-6.6
Ph₃SnL3							
BCP-1	0.112	0.109	201.6	-332.0	-130.4	0.61	-166.0
BCP-2	0.110	0.110	197.7	-323.5	-125.7	0.61	-161.7
BCP-3	0.110	0.115	203.5	-331.5	-128.0	0.61	-165.7
BCP-4	0.094	0.398	306.1	-351.2	-45.1	0.87	-175.6
BCP-1'	0.007	0.026	14.6	-12.0	2.6	1.22	-6.0
BCP-2'	0.011	0.039	22.5	-19.6	2.9	1.15	-9.8

Table S5. The experimental and theoretical wavelengths (cm^{-1}) and PED (%) analysis parameters for **Ph₃SnL1**.

Assignments of Ph ₃ SnL1	Exp. values	B3LYP-D3BJ/6-311++g(d,p)/def2-TZVPD	
	IR (cm^{-1})	Calculated (cm^{-1})	PED (%) of Ph ₃ SnL1
C-H stretching (Ph)/ C-H stretching (-CH ₃)	3046	3131	ν_{CH} (99)
C-H stretching (-CH ₂ -)	2988	2976	ν_{HC} (99)
C=O3 stretching/ C-H stretching (-CH ₂ -)	1640	1688	$\nu_{\text{C=O3}}$ (63) + ν_{CC} (11)
C=O2 stretching	1553	1614	$\nu_{\text{C=O1}}$ (84)
H-C-H bending (quinoline ring) C-C-H bending (quinoline ring)	1429	1455	δ_{HCH} (40) + δ_{CCH} (20)
C=O1 stretching/ C-C stretching	1333	1305	$\nu_{\text{C=O2}}$ (40) + $\nu_{\text{C-C}}$ (18)
H-C-C bending/ C-C-H bending/ C-C stretching (Ph)	1077	1073	δ_{HCH} (30) + δ_{CCH} (20) + ν_{HC} (10)
C-C-H bending/ H-C-C-H torsion (w.t) (Ph)	998	945	δ_{CCH} (31) + τ_{HCC} (10)
H-C-C-H torsion (w.t) (Ph)/ C-C-C-H torsion (w.t) (Ph)	730	730	τ_{HCC} (21) + τ_{CCC} (17)
N-C-C-H torsion (w.t) (quinoline ring) C-N-C-O torsion (w.t) (quinoline ring)	697	698	τ_{NCCH} (12) + τ_{CNCO} (19)
Sn-O1 stretching/ O-C-C bending (quinoline ring)	452	450	$\nu_{\text{Sn-O2}}$ (21) + δ_{OCC} (30)
C-Sn stretching/ C-C-C bending	274	270	$\nu_{\text{C-Sn}}$ (43) + δ_{CCC} (10)

Table S6. The experimental and theoretical wavelengths (cm^{-1}) and PED (%) analysis parameters for **Ph₃SnL2**.

Assignments of Ph ₃ SnL2	Exp. values	B3LYP-D3BJ/6-311++g(d,p)/def2-TZVPD	
	IR (cm^{-1})	Calculated (cm^{-1})	PED (%) of Ph ₃ SnL2
C-H stretching (Ph)/ C-H stretching (-CH ₃)	3045	3143	ν_{CH} (99)
C-H stretching (-CH ₂ -)	2989	3043	ν_{HC} (91)
C=O3 stretching	1660	1699	$\nu_{\text{C=O3}}$ (95)
C=O2 stretching	1559	1619	$\nu_{\text{C=O1}}$ (80)
H-C-H bending (quinoline ring, -CH ₃) C-C-H bending (quinoline ring)	1428	1463	δ_{HCH} (38) + δ_{CCH} (20)
C=O1 stretching/ C-C stretching	1305	1327	$\nu_{\text{C=O1}}$ (31) + ν_{CC} (14)
C-C-H bending/ H-C-C-H torsion (w.t) (Ph)	1077	1080	δ_{CCH} (60) + τ_{HCC} (11)
C-C-C-H torsion (w.t) (Ph) H-C-C-C torsion (w.t) (Ph)	730	730	τ_{HCC} (20) + τ_{HCCC} (28)
Sn-O1 stretching/ N-C-C bending (quinoline ring)	455	452	$\nu_{\text{Sn-O2}}$ (16) + δ_{NCC} (18)
C-Sn stretching/ Sn-C-C bending	277	276	$\nu_{\text{C-Sn}}$ (50) + δ_{CCC} (6)

Table S7. The experimental and theoretical wavelengths (cm^{-1}) and PED (%) analysis parameters for $\text{Ph}_3\text{SnL3}$.

Assignments of $\text{Ph}_3\text{SnL3}$	Exp. values	B3LYP-D3BJ/6-311++g(d,p)/def2-TZVPD	
	IR (cm^{-1})	Calculated (cm^{-1})	PED (%) of $\text{Ph}_3\text{SnL3}$
O-H stretching	3719	3744	ν_{OH} (100)
C-H stretching (Ph)/ C-H stretching ($-\text{CH}_3$)	3045	3142	ν_{CH} (99)
C-H stretching ($-\text{CH}_2-$)	2990	3031	ν_{CH} (99)
C=O3 stretching	1638	1695	$\nu_{\text{C=O2}}$ (70)
C=O2 stretching	1556	1513	$\nu_{\text{C=O1}}$ (85)
C-C-H bending (quinoline ring)	1428	1438	δ_{CCH} (80)
C=O1 stretching/ C-C stretching	1334	1331	$\nu_{\text{C=O2}}$ (35) + $\nu_{\text{C-C}}$ (11)
C-C-H bending/ C-C stretching (Ph)	1076	1075	δ_{CCH} (25) + ν_{CC} (15)
CCCH torsion (w.t) (Ph) HCCH torsion (w.t) (Ph)	729	730	τ_{HCCH} (40) + τ_{CCCH} (28)
NCCH torsion (w.t) (quinoline ring) CNCO torsion (w.t) (Ph)	695	697	τ_{NCCH} (10) + τ_{CNCO} (8)
Sn-O1 stretching/ N-C-C bending (quinoline ring)	452	451	$\nu_{\text{Sn-O2}}$ (30) + δ_{NCC} (10)
C-Sn stretching/ Sn-C-C bending	273	273	$\nu_{\text{C-Sn}}$ (26) + δ_{SnCC} (10)

Table S8. The experimental and calculated chemical shifts (ppm) in the ^1H NMR spectra of triphenyltin(IV) complexes.

Atoms	$\text{Ph}_3\text{SnL1},$ δ (ppm)		$\text{Ph}_3\text{SnL2},$ δ (ppm)		$\text{Ph}_3\text{SnL3},$ δ (ppm)		
	Exp.	Theor.	Exp.	Theor.	Exp.	Theor.	
						${}^{\text{IV}}\text{Ph}_3\text{SnL}_3$	${}^{\text{V}}\text{Ph}_3\text{SnL}_3$
$-\text{CH}_3/\text{OH} (\text{C-H}^{14/13})$	2.44	2.00	2.43	2.63		-	-
C-H^{12}	2.84	3.26	5.12	5.21	4.8	5.10	4.84
C-H^{13}	4.61	4.54	-	-	-	-	-
C-H^3	6.54	6.64	6.51	6.94	5.74	5.86	5.65
C-H^7	7.21	6.39	7.19	6.01	7.22	6.28	6.33
C-H^8	7.42	7.91	6.92	6.88	7.22	6.84	6.58
C-H^p	7.46	7.72	7.40	7.74	7.36	7.88	7.80
C-H^m	7.46	7.65	7.40	7.77	7.36	7.44	7.75
C-H^6	7.68	6.81	7.25	6.91	6.92	7.33	7.42
C-H^o	7.73	7.89	7.63	7.75	7.67	7.51	7.60
C-H^5	7.79	6.84	7.68	7.63	8.01	8.41	8.39
MAE	0.43		0.32		0.34		0.39
R	0.965		0.958		0.897		0.905

Table S9. The experimental and calculated chemical shifts (ppm) in the ^{13}C NMR spectra of triphenyltin(IV) complexes.

Atoms	Ph_3SnL_1 , δ (ppm)		Ph_3SnL_2 , δ (ppm)		Ph_3SnL_3 , δ (ppm)		
	Exp.	Theor.	Exp.	Theor.	Exp.	Theor. $^{\text{IV}}\text{Ph}_3\text{SnL}_3$	Theor. $^{\text{V}}\text{Ph}_3\text{SnL}_3$
-CH₃ (C14/13)	18.3	21.0	18.5	22.0	-	-	-
C12	31.6	35.2	43.4	48.0	43.2	48.5	48.0
C13	38.0	43.0	-	-	-	-	-
C8	113.7	114.2	113.9	109.7	113.6	112.6	112.4
C3	120.4	119.6	120.0	118.3	94.1	95.8	96.9
C10	121.1	116.6	120.9	120.3	116.1	113.8	114.4
C6	121.3	118.2	121.5	119.4	121.0	119.0	119.6
C5	124.8	124.5	124.7	120.9	122.7	121.0	120.9
C-m	129.8	125.5	129.6	125.7	128.4	126.2	126.2
C-p	128.6	127.2	128.3	127.7	127.6	126.8	128.1
C7	129.8	128.8	129.8	127.8	130.6	129.4	129.5
C-o	136.2	134.5	136.0	133.8	135.4	133.5	134.1
C9	138.1	136.5	138.5	134.9	138.8	138.6	138.2
C-i	135.6	135.3	135.6	134.8	139.8	135.1	138.3
C4	146.0	147.9	146.7	147.2	162.4	159.0	158.3
C2	161.1	158.7	161.1	157.7	164.0	159.9	160.1
C11	176.9	177.0	173.1	173.3	171.3	171.7	173.5
MAE	2.22		2.36		2.19		1.99
R	0.999		0.999		0.998		0.999

Table S10. Crystal data and structure refinement for **Ph₃SnL1** and **Ph₃SnL2**.

Empirical formula	Ph₃SnL1 (C₃₁H₂₇NO₃Sn)	Ph₃SnL2 (C₃₀H₂₅NO₃Sn)
Formula weight	580.22	566.20
Temperature	100 K	100 K
Wavelength	0.71073 Å	0.71073 Å
Crystal system	Monoclinic	Monoclinic
Space group	P2 ₁ /n	P2 ₁ /c
a	17.6237(4) Å	9.9429(1) Å
b	15.5051(3) Å	13.8691(2) Å
c	19.1439(5) Å	17.5691(3) Å
α, β, γ (°)	90 °, 96.914(2) °, 90°	90 °, 92.210(2) °, 90 °
Volume	5193.2(2) Å ³	2420.96(6) Å ³
Z	8	4
Calculated density	1.484 mg/mm ³	1.553 mg/mm ³
Absorption coefficient	1.017 mm ⁻¹	1.088 mm ⁻¹
F(000)	2352	1144
Crystal size	0.43 × 0.38 × 0.11 mm	0.4 × 0.4 × 0.34 mm
θ range for data collection	3.116 to 28.958 deg.	3.037 to 29.105 deg.
Limiting indices	-22<=h<=23, -20<=k<=19, -24<=l<=25	-13<=h<=13, -18<=k<=18, -22<=l<=24
Reflections collected / unique	71496 / 12290 [R _{int} = 0.0875]	28772 / 5900 [R _{int} = 0.0335]
Completeness to θ = 25.242	99.8 %	99.8 %
Absorption correction	Analytical	Semi-empirical from equivalents
Max. and min. transmission	0.920 and 0.714	1.00000 and 0.96529
Refinement method	Full-matrix least-squares on F ²	Full-matrix least-squares on F ²
Data / restraints / parameters	12290 / 0 / 650	5900 / 0 / 317
Goodness-of-fit on F²	1.046	1.027
Final R indices [I>2σ(I)]	R ₁ = 0.0412, wR ₂ = 0.0988	R ₁ = 0.0230, wR ₂ = 0.0501
R indices (all data)	R ₁ = 0.0533, wR ₂ = 0.1119	R ₁ = 0.0296, wR ₂ = 0.0531

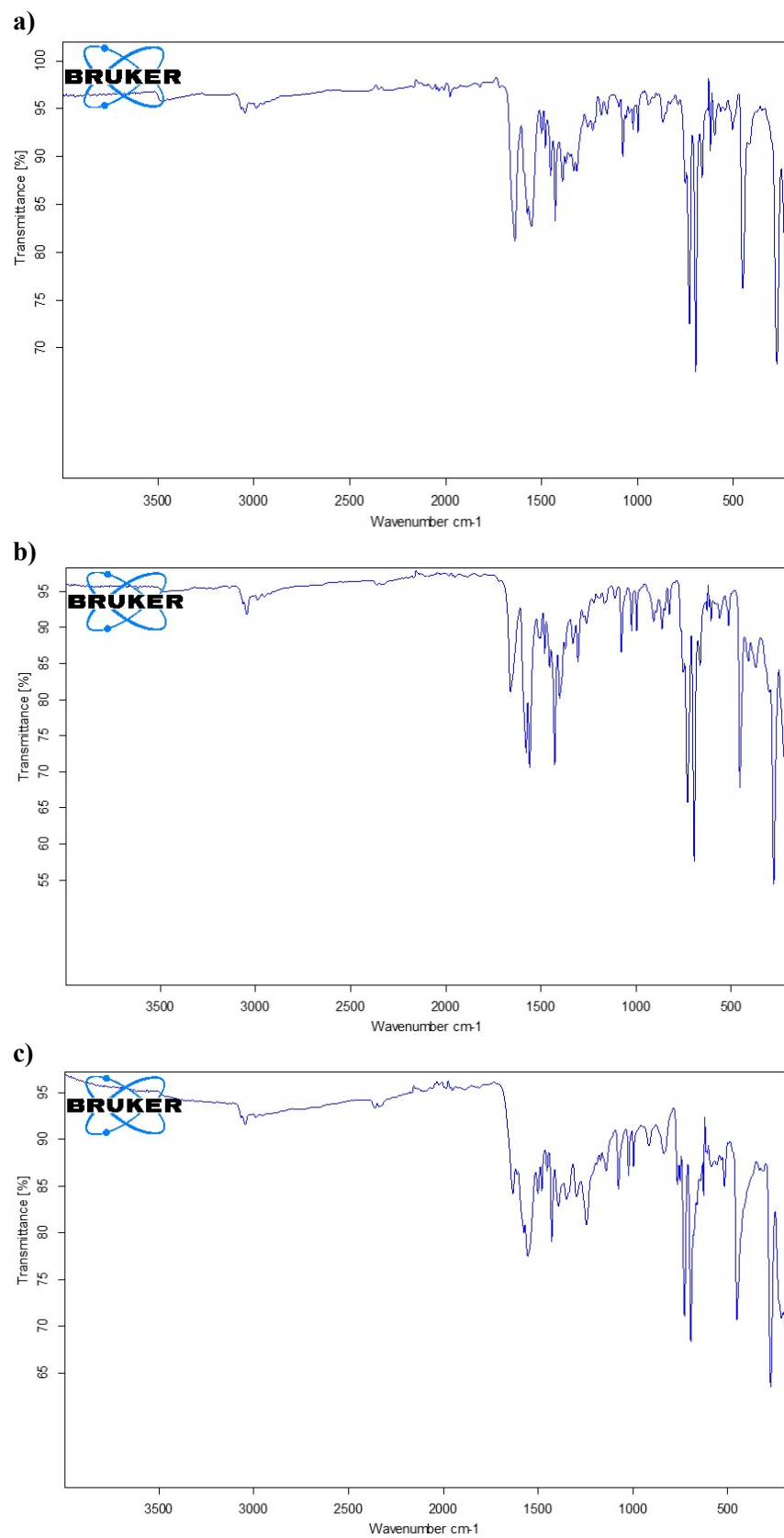


Figure S1. FT-IR spectra of the triphenyltin(IV) compounds: a) **Ph₃SnL1**, b) **Ph₃SnL2**, c) **Ph₃SnL3**.

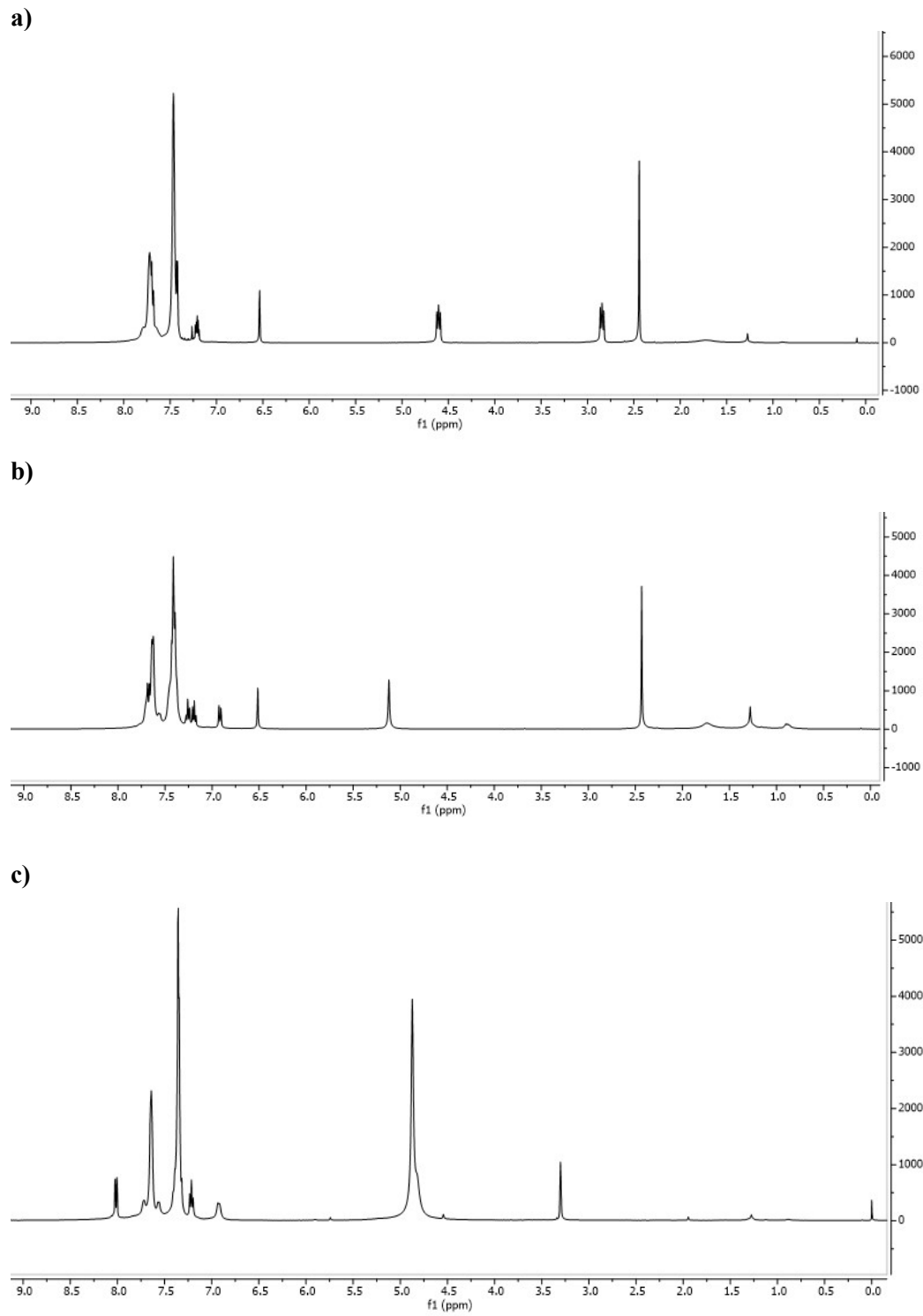


Figure S2. ^1H NMR of triphenyltin(IV) compounds: a) **Ph₃SnL1**, b) **Ph₃SnL2**, c) **Ph₃SnL3**.

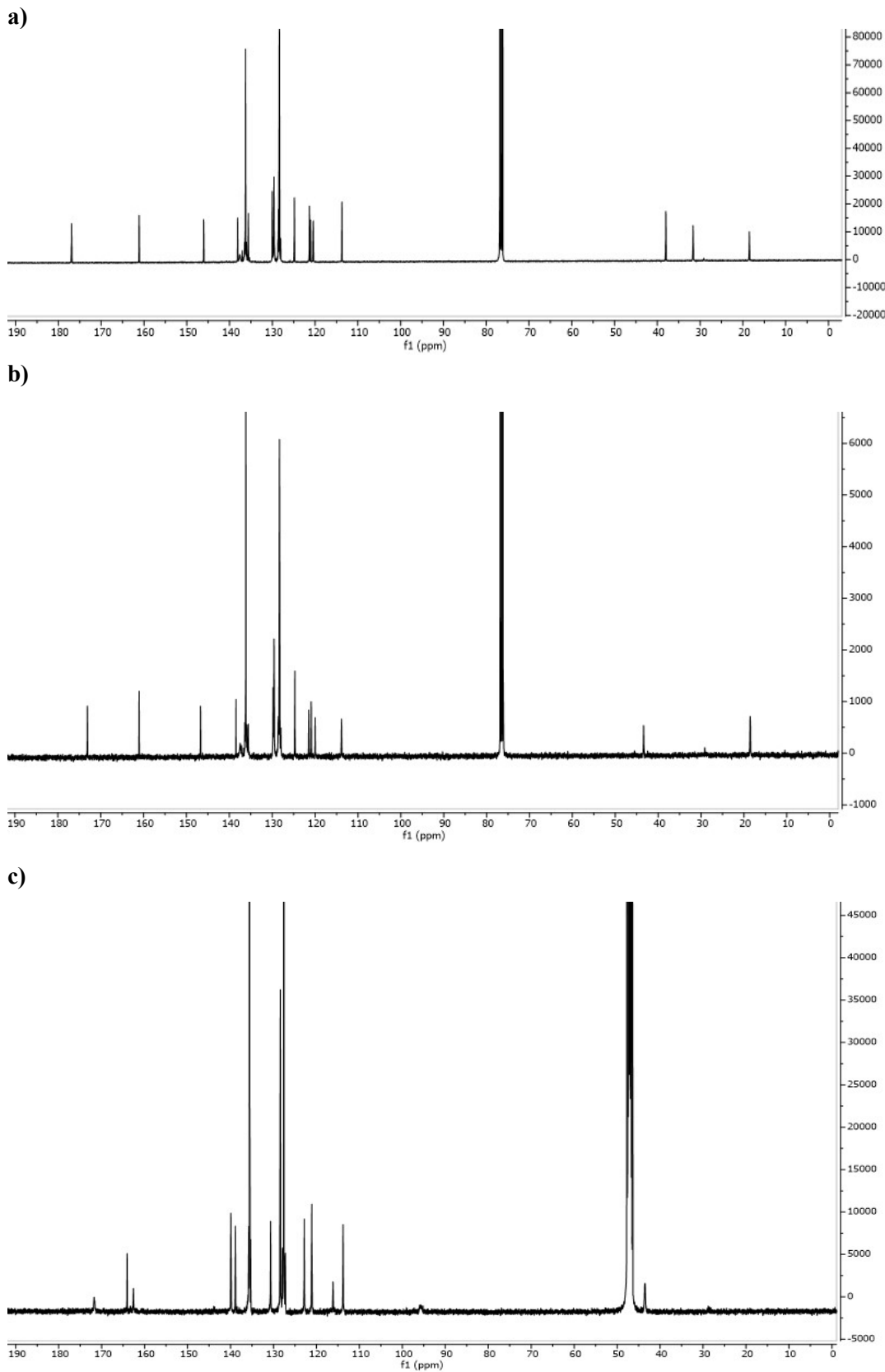


Figure S3. ^{13}C NMR of triphenyltin(IV) compounds: a) **Ph₃SnL1**, b) **Ph₃SnL2**, c) **Ph₃SnL3**.

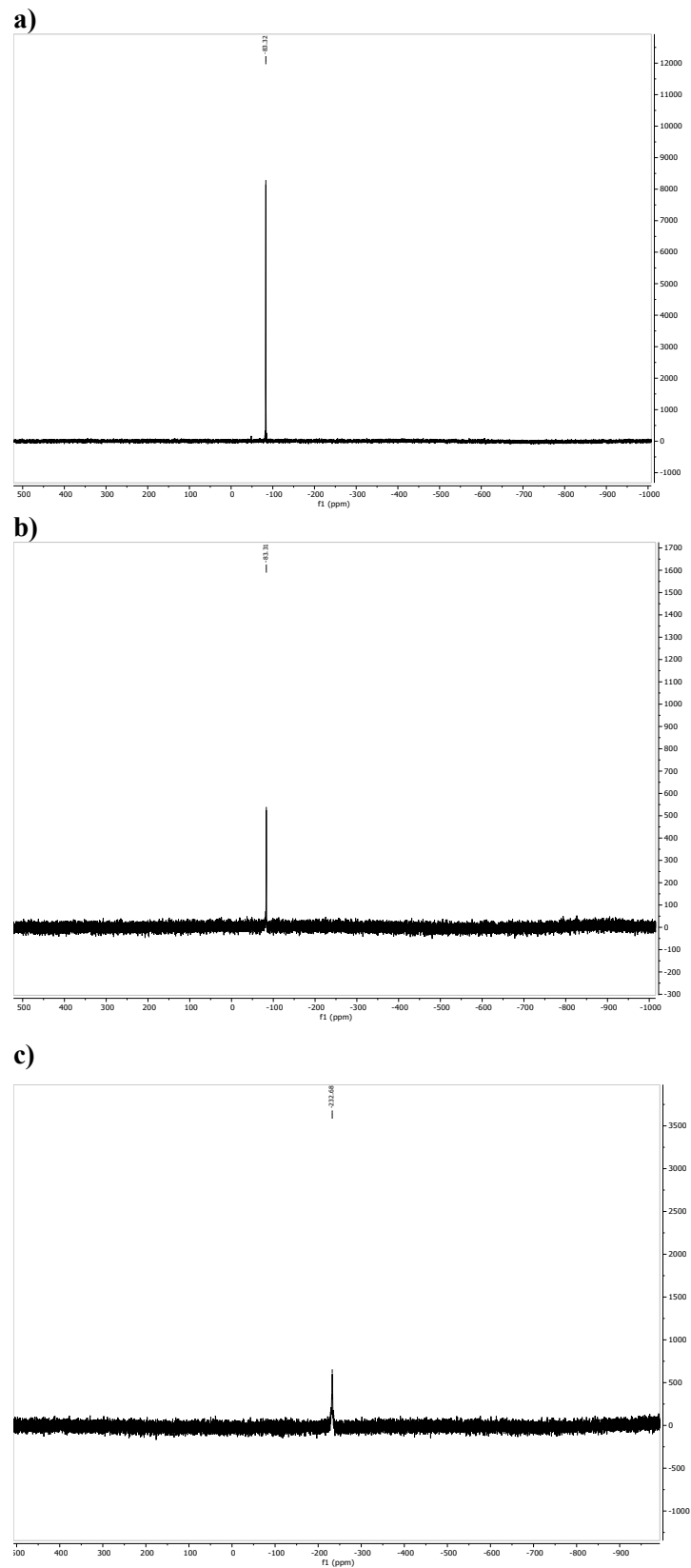


Figure S4. ^{119}Sn NMR of triphenyltin(IV) compounds: a) **Ph₃SnL1**, b) **Ph₃SnL2**, c)

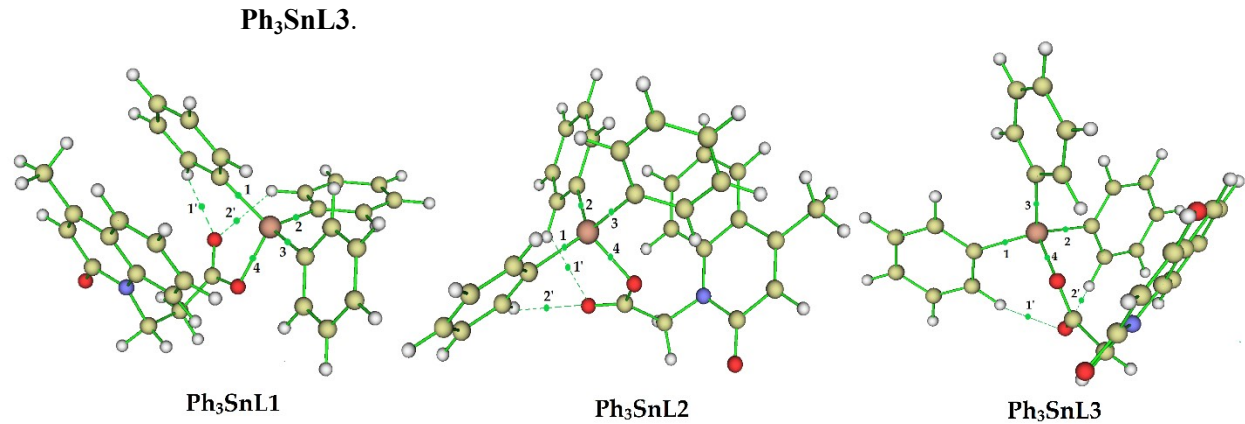


Figure S5. Structures of newly synthesized compounds with defined characteristics and numbered Bond Critical Points (BCP) obtained by using QTAIM analysis.

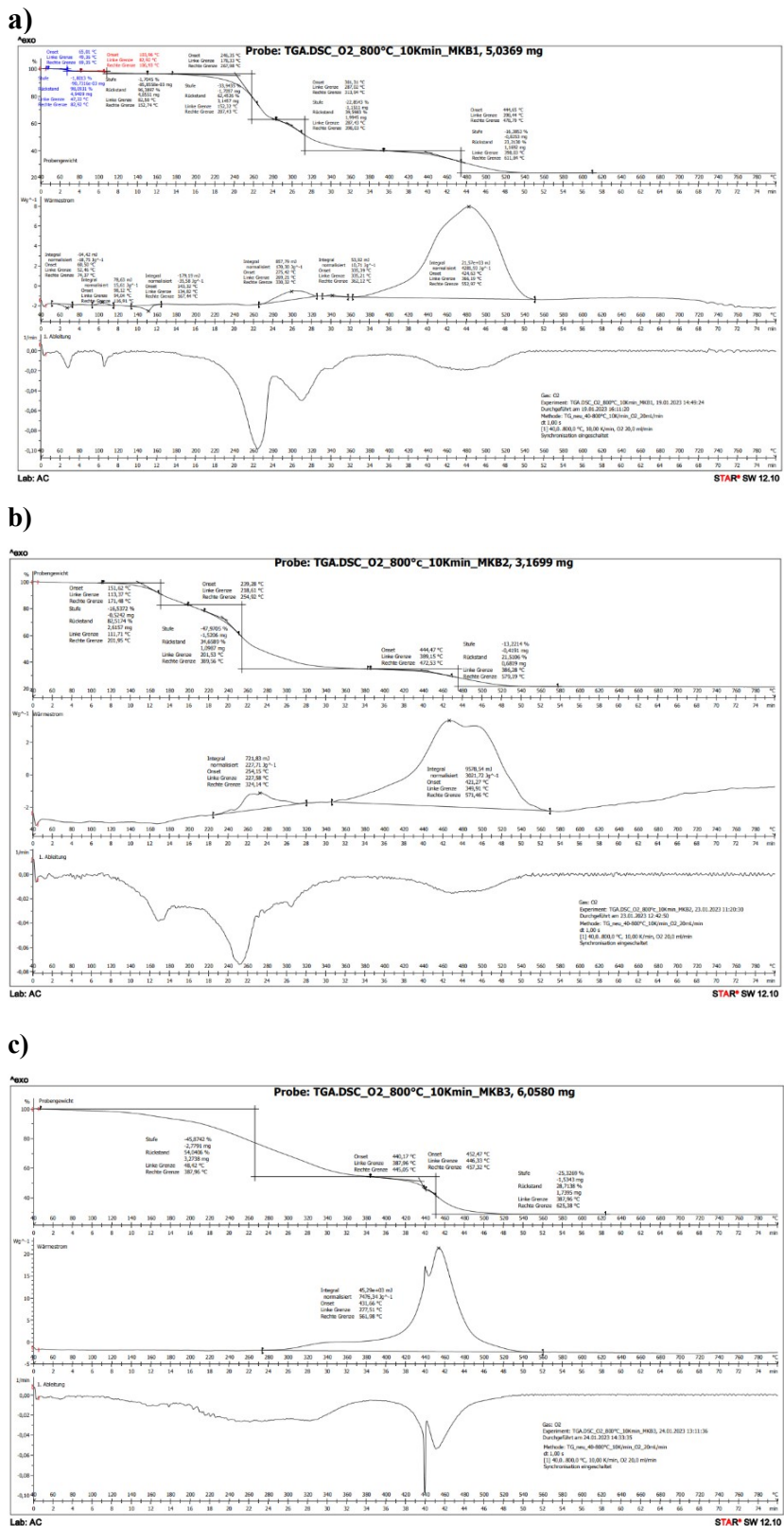


Figure S6. Thermogravimetric analyses carried out in a non-inert atmosphere (O_2):
a) $\text{Ph}_3\text{SnL1}$, b) $\text{Ph}_3\text{SnL2}$, c) $\text{Ph}_3\text{SnL3}$.

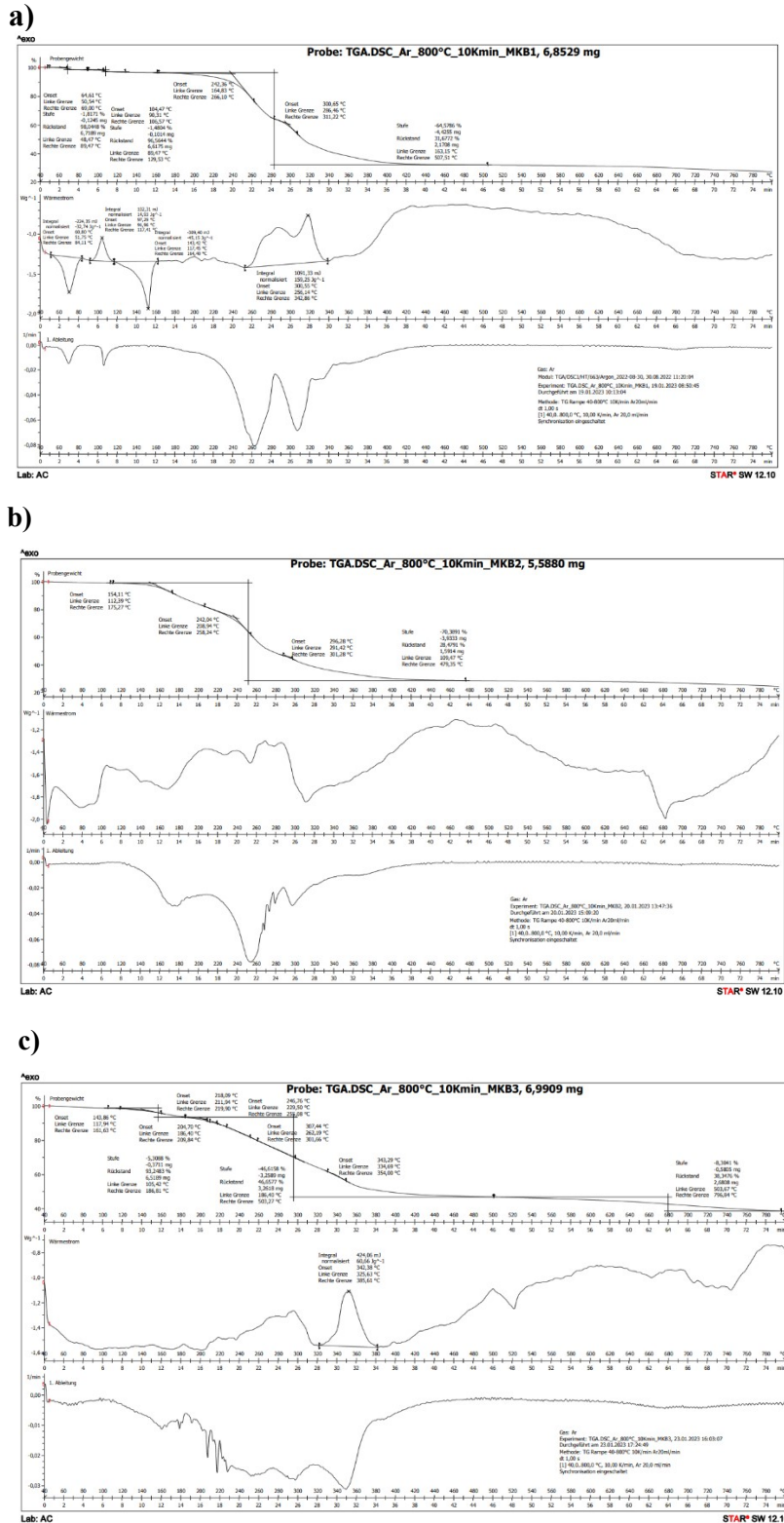


Figure S7. Thermogravimetric analyses carried out in an inert (Ar) atmosphere:
 a) $\text{Ph}_3\text{SnL1}$, b) $\text{Ph}_3\text{SnL2}$, c) $\text{Ph}_3\text{SnL3}$.

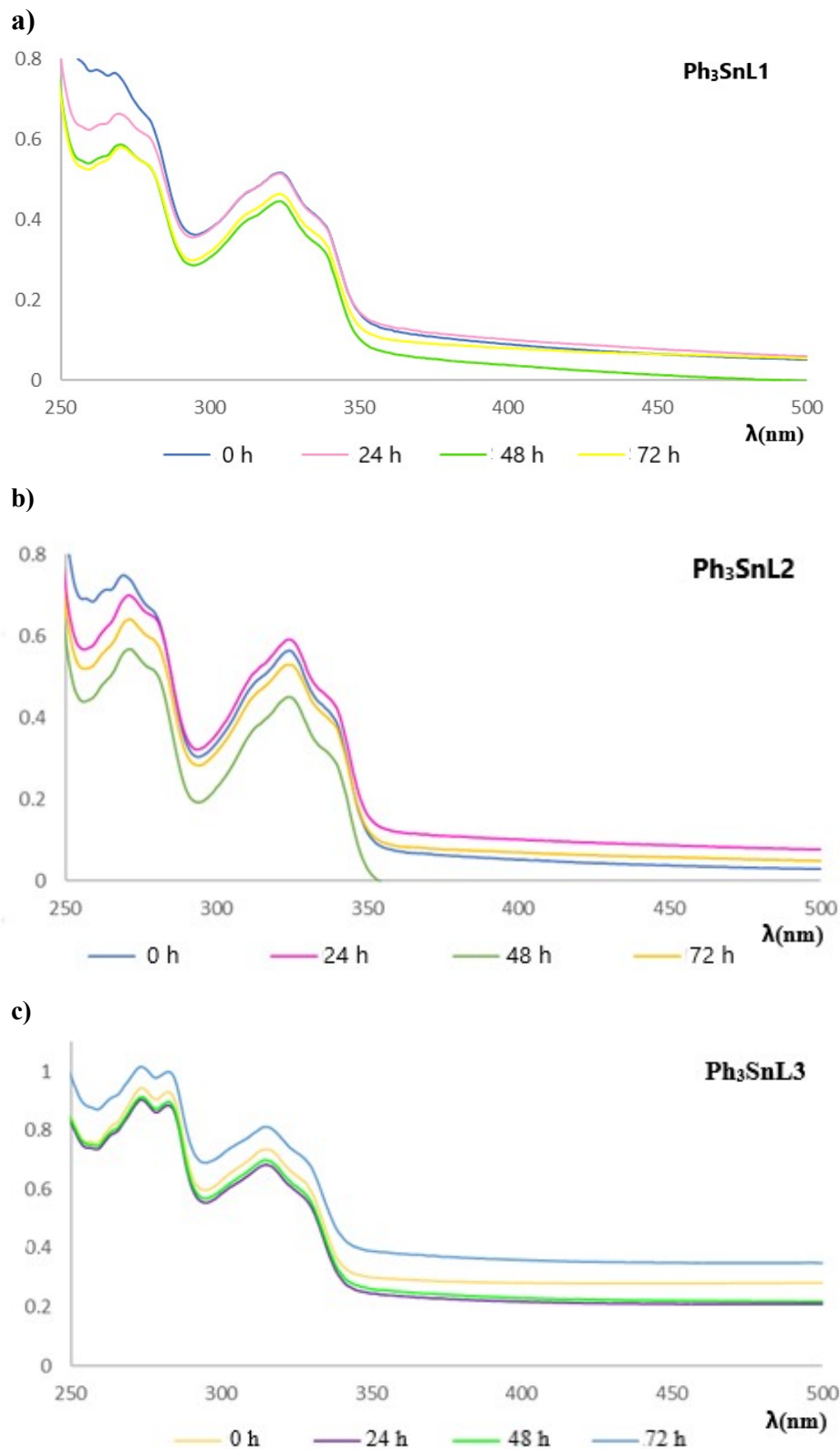


Figure S8. UV-Vis spectra of triphenyltin(IV) compounds in water/DMSO solution, immediately after dissolution and after 24, 48 and 72 h : a) **Ph₃SnL1**, b) **Ph₃SnL2**, c) **Ph₃SnL3**.

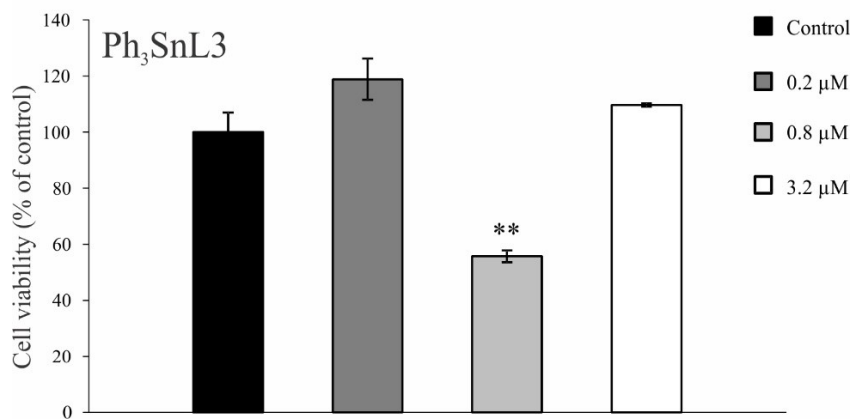
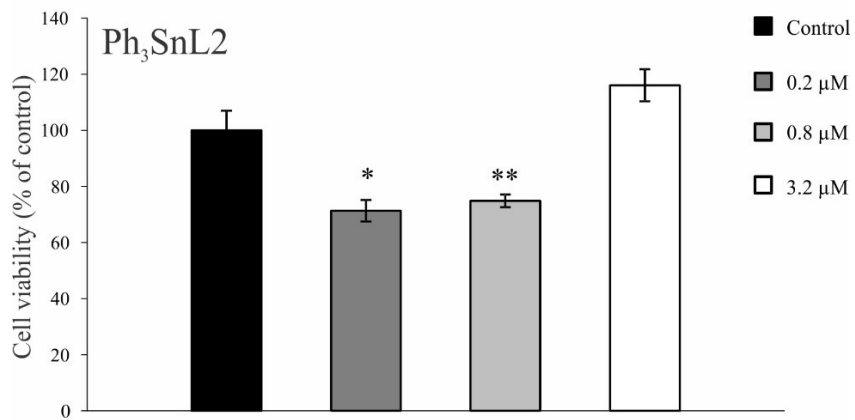
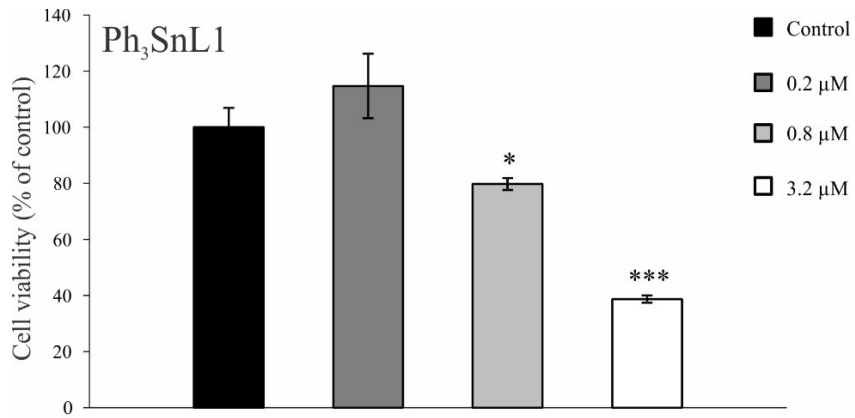


Figure S9. The effect of compounds **Ph₃SnL1**, **Ph₃SnL2** and **Ph₃SnL3** on viability of peritoneal exudate cells. PEC were exposed to selected drug for 72 h and MTT and CV assays were performed. All data presented on the figure represent mean \pm SD of three independent experiments and are expressed as percentage of untreated cells (arbitrary set as 100%). ** p < 0.01 and *** p < 0.001.

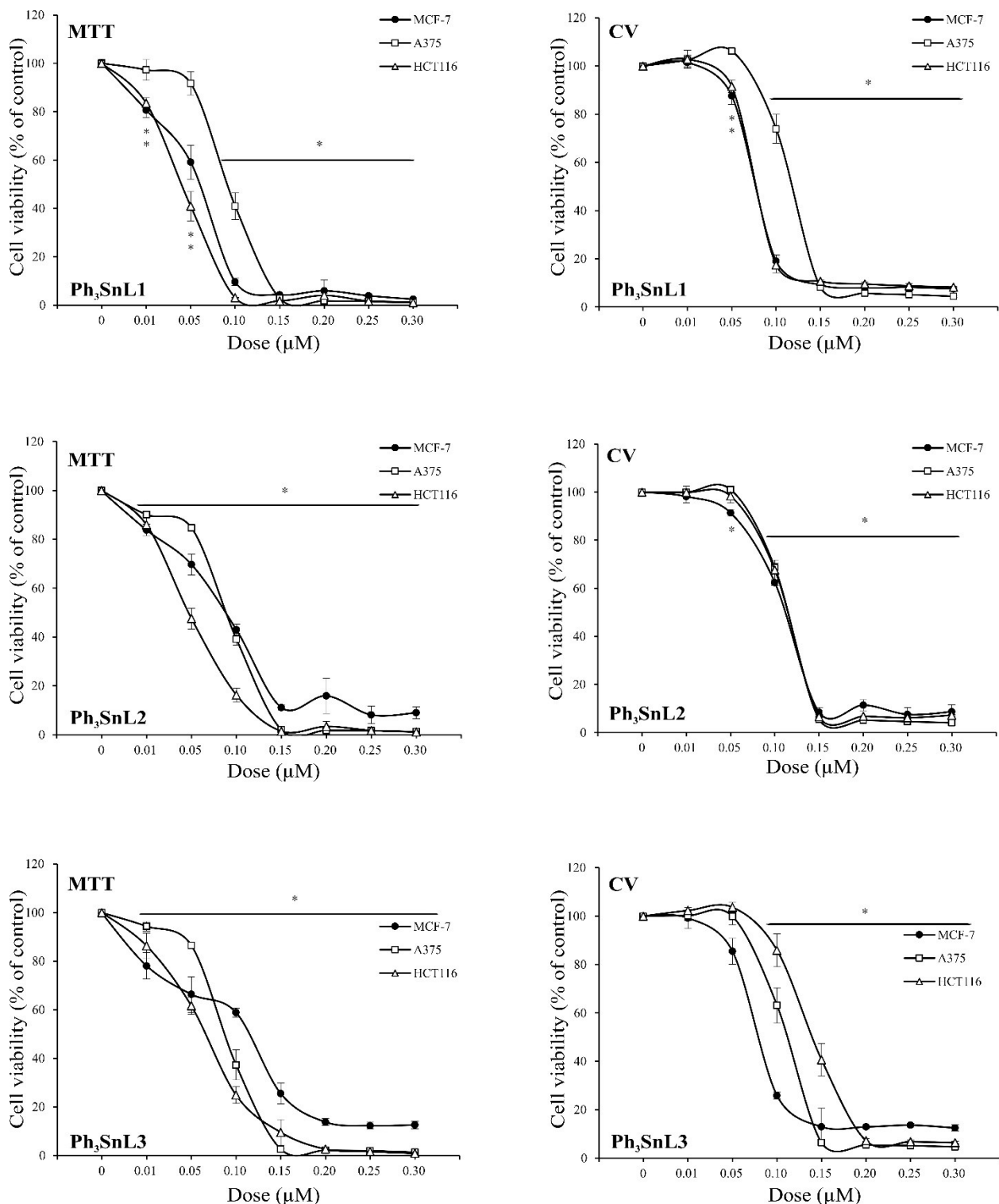


Figure S10. Compounds **Ph₃SnL1**, **Ph₃SnL2** and **Ph₃SnL3** decreased cell viability of human cancer cell lines. Cell lines were treated with experimental compounds for 72 h and MTT and CV assays were performed. All data are expressed as mean \pm SD of one representative of three independent experiments. Statistically significant were considered *p* values of less than 0.05 (*).

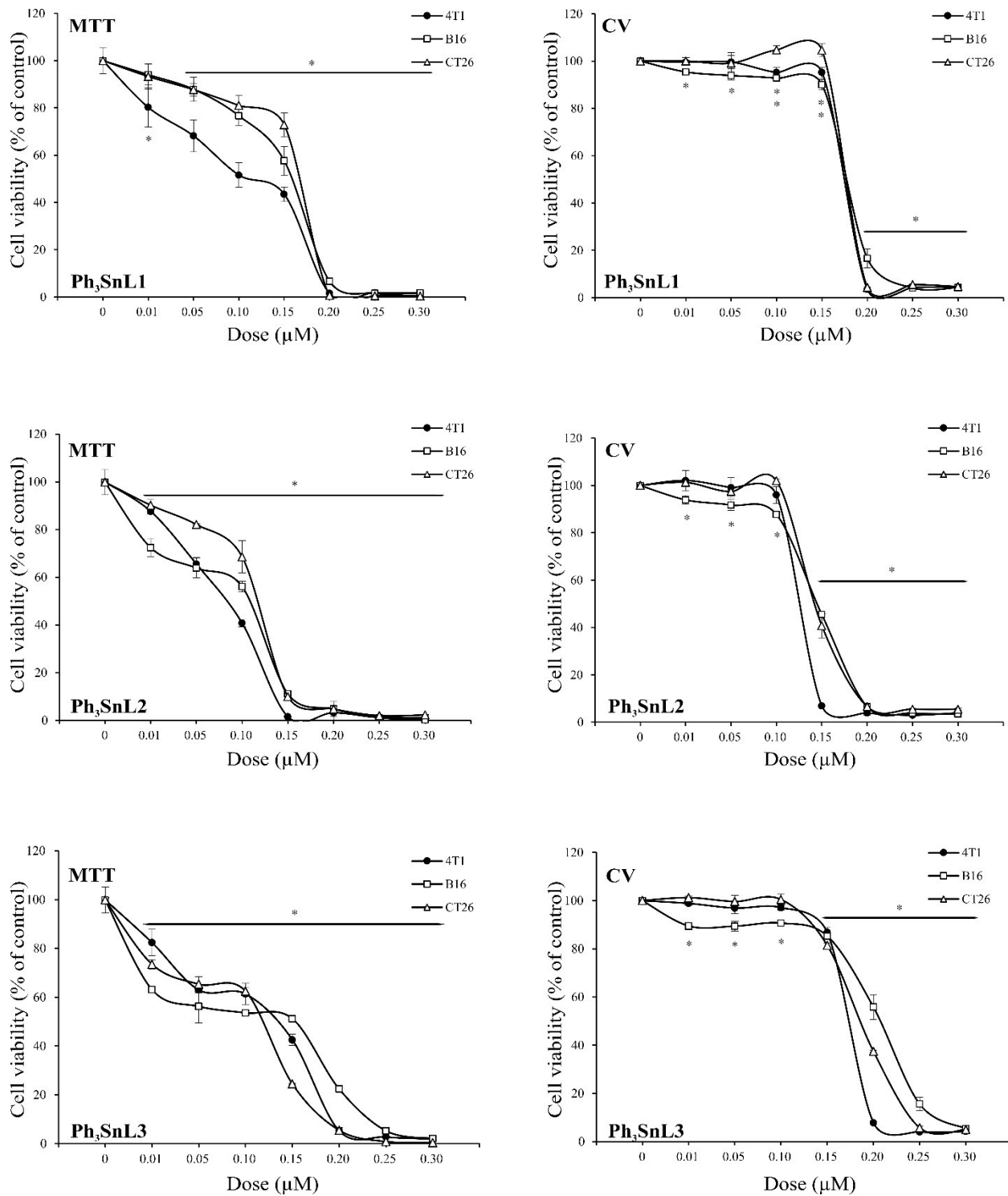


Figure S11. Compounds **Ph₃SnL1**, **Ph₃SnL2** and **Ph₃SnL3** decreased cell viability of mouse cancer cell lines. Cell lines were treated with experimental compounds for 72 h and MTT and CV assays were performed. All data are expressed as mean \pm SD of one representative of three independent experiments. Statistically significant were considered p values of less than 0.05 (*).

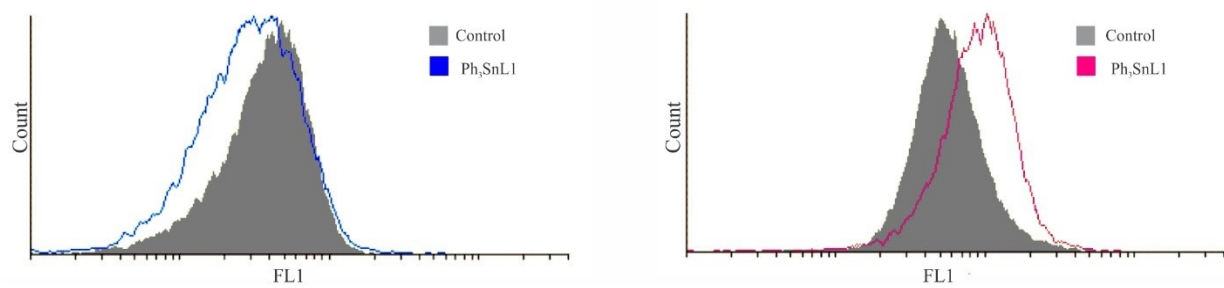


Figure S12. Compound **Ph₃SnL1** exhibited different effects on production of ROS/RNS in A375 and B16 cells. Cells were prestained with DHR 123 staining and exposed to IC₅₀ value of compound **Ph₃SnL1** for 24 h and analyzed by flow cytometry. (Left panel) A375; (Right panel) B16.